JOURNAL OF THERMOPHYSICS AND HEAT TRANSFER
Vol. 6, No. 4, Oct.–Dec. 1992

Analytic Solution of the Transient Behavior of Radiation-Backscattering Heat Shields

Charles J. Cornelison* and John T. Howe†
NASA Ames Research Center, Moffet Field, California 94035

An analytic solution of the material response to combined radiative and convective heating is presented. The solution includes the equations of radiative transfer (within the material), coupled to a transient energy equation that contains both radiative and convective terms. The analysis allows for unlimited spectral detail, but assumes that within the range of applicability, the various material properties do not vary significantly with temperature. To facilitate development of the analytic solution, it is also assumed that scattering within the material dominates absorption, and that the exposed surface of the material does not ablate. The exposed surface boundary condition includes convective heating and spectral radiation, some of which is absorbed by the surface and some of which penetrates the surface.

Nomenclature

A = transformed value of a, Eq. (21)
a = radius of the inner surface
B = transformed value of b, Eq. (22)
b = radius of the exposed surface
C_n = series coefficient for the general solution
$\bar{C}_1$ = material property const, Eq. (8)
$\bar{C}_2$ = material property const, Eq. (9)
c_p = specific heat of solid
f_b = boundary condition flux term, Eq. (26)
I = bidirectional radiative intensity
K = bidirectional absorption coefficient
k = thermal conductivity
m = geometric superscript, Eq. (2)
n = index of refraction
q_b = surface emitted radiative flux
q_c = conductive heat flux within the material
q_e = radiative flux that penetrates the surface
q_r = total radiative flux
q_{SNP} = radiative flux that does not penetrate the surface
q_w = convective heat flux incident on the material surface
R = overall reflectance
R_e = reflectance of the exposed surface to the incident radiative flux
R_i = internal reflectance of the exposed surface to the outward-bound radiative flux
R_s = reflectance of the substrate backing of the heat shield
r = radial distance to a layer within the heat shield
S = bidirectional scattering coefficient
T = temperature
t = time
y = coordinate measured outward from the rear surface
Z = transformed value of r, Eq. (20)
α = defined by Eq. (24)
β = defined by Eq. (25)
δ = heat shield thickness, $b-a$
λ_n = eigenvalue
ρ = heat shield material density
Φ = transformed temperature
Ψ = steady-state temperature

Subscripts
b = black body condition; location where $r = b$
j = jth spectral band of surface nonpenetrating radiation
o = initial condition
R = outward-bound (reflected) direction
T = inward-bound (transmitted) direction
t = derivative with respect to time
z = derivative with respect to Z
ν = νth spectral band of surface penetrating radiation

Introduction

DURING the early 1970s the challenge to develop thermal protective materials that could withstand severe radiation-dominated heating environments received considerable attention. These studies led to the concept of a backscattering or volume-reflecting heat shield.[1] The basic idea was to construct a heat shield from material that would act as a mirror (in the depths of the material) to the predominant radiative heating component. Primarily, only the convective heating component, and part of the radiative flux absorbed on the surface, would actually be absorbed by the protective material. As a result, the size and weight of a backscattering-type heat shield would be expected to be substantially less than that of a conventional ablative type. Although a quarter-scale model of a Jovian heat shield was developed, the effort was terminated for nontechnical reasons. Several proposed space programs are anticipated to experience significant radiative heating, however, and interest in this potentially useful concept has been rekindled.

A volume-reflecting heat shield material is basically a window to the spectral radiative flux of interest, i.e., a material that transmits almost all, yet absorbs very little, of the incident radiation. The material is pulverized into a fine powder with optimum particle sizes determined by scattering theory.[2] This powder is then reformed into a solid material, that is composed of particles that are densely packed radiation-scattering sites.

Presented as Paper 91-1322 at the AIAA 26th Thermophysics Conference, Honolulu, HI, June 24–26, 1991; received July 31, 1991; revision received Nov. 11, 1991; accepted for publication Nov. 13, 1991.

*Research Scientist, Thermoscience Division, M/S 229-4.
†Senior Staff Scientist, Thermoscience Division, M/S 229-4. Fellow AIAA.

Depending on the material thickness and the magnitude of the radiative flux, the majority of the incident radiation will be either reflected (backscattered in depth) or transmitted, and very little will be absorbed. A naturally occurring example of this phenomenon is a snowbank exposed to the visible portion of the radiative spectrum. Snow under these conditions appears white, and doesn't melt appreciably, because it backscatters virtually all of the incident radiation and absorbs very little of it. Thus it would appear, that materials best suited for the backscattering, thermal-protective application, are ones that display high-scattering and low-absorption behavior.

Analysis

To begin the analysis, a heat shield of arbitrary geometry exposed to both a convective heat flux, q_w, and a monochromatic radiative flux, q_r (that penetrates the material to be backscattered, absorbed, etc., in depth), will be considered. Subsequently, the analysis will be generalized to accommodate spectral variability. The radiative flux will be split into surface-penetrating and nonpenetrating components. The spectral bands that penetrate will be treated in an analogous manner to the monochromatic flux. However, the nonpenetrating bands (which are either reflected or absorbed at the exposed surface) will be coupled with the convective flux as part of the exposed-surface boundary condition.

Radiative Transfer

Two ordinary differential equations that describe the radiative transfer within a backscattering material are the Kubelka-Munk equations,[3] that have been modified to allow for emission. These equations, for an inwardly and outwardly directed radiative intensity I, are, respectively

$$\frac{1}{r^m}\frac{\mathrm{d}}{\mathrm{d}r}(r^m I_T) = (K + S)I_T - SI_R - Kn^2 I_b \tag{1}$$

$$\frac{1}{r^m}\frac{\mathrm{d}}{\mathrm{d}r}(r^m I_R) = -(K + S)I_R + SI_T + Kn^2 I_b \tag{2}$$

where the geometric constant is

$m = 0$ flat plate

$m = 1$ cylinder

$m = 2$ sphere

Notice that the outward-bound intensity (I_R) is diminished by absorption and scattering, but is enhanced by emission and the scattered portion of the inward-bound intensity (I_T). The inward-bound intensity is altered in a similar fashion, but in the opposite direction (see Fig. 1). A parallel development that has been documented by Howe and Yang[4] employs the astrophysical work of Schuster,[5] and yields similar expressions. In fact, Ref. 4 presents a derivation that relates and equates these two developments.

These radiative transfer expressions can be simplified somewhat by recognizing that strongly scattering and weakly absorbing behavior typifies materials that are well suited for this application. In other words, for materials of interest

$$S >> K \tag{3}$$

Furthermore, for severe heating environments (i.e., shock-layer temperature on the order of 15,000 K) the incident radiative flux is much larger than the flux emitted from the relatively cooler material. It would therefore, be expected that the magnitude of the net scattered intensity would be much larger than the intensity resulting from emission, therefore

$$S(I_T - I_R) >> Kn^2 I_b \tag{4}$$

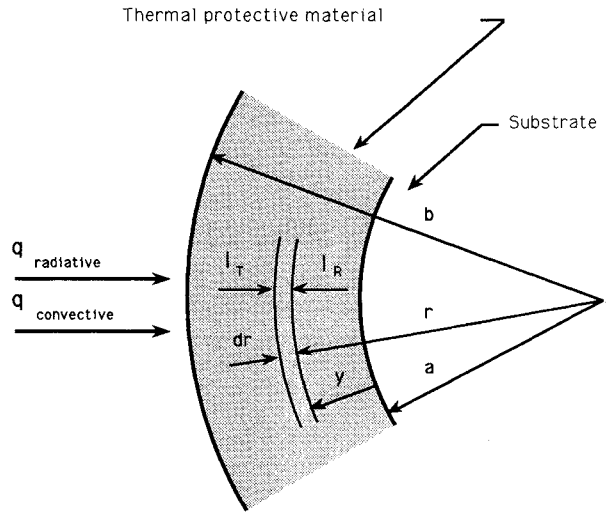

Fig. 1 Generic heat shield configuration.

Thus, for materials and conditions of interest the radiative transfer equations can be reduced to

$$\frac{\mathrm{d}}{\mathrm{d}r}(r^m I_T) = \frac{\mathrm{d}}{\mathrm{d}r}(r^m I_R) = r^m S(I_T - I_R) \tag{5}$$

Solving these simplified differential equations yields

$$I_T = \frac{b^m}{r^m}[\bar{C}_2 + S\bar{C}_1(y + a)] \tag{6}$$

$$I_R = \frac{b^m}{r^m}[\bar{C}_2 - \bar{C}_1 + S\bar{C}_1(y + a)] \tag{7}$$

where

$$\bar{C}_1 = \frac{(q_e/\pi)(1 - R_e)(1 - R_s)}{\{(1 - R_i)[1 + (1 - R_s)S\delta] + R_i(1 - R_s)\}} \tag{8}$$

$$\bar{C}_2 = \frac{(q_e/\pi)(1 - R_e)[1 - (1 - R_s)Sa]}{\{(1 - R_i)[1 + (1 - R_s)S\delta] + R_i(1 - R_s)\}} \tag{9}$$

Note that q_e is the incident flux that penetrates the surface.

Energy Equation

Performing an energy balance[6] on the heat shield material element dr (see Fig. 1) yields

$$\rho c_p \frac{\partial T}{\partial t} = -\frac{1}{r^m}\frac{\partial}{\partial r}[(q_c + q_r)r^m] \tag{10}$$

By assuming that the various material properties (k, c_p, S_ν, K_ν, etc.) do not vary significantly with temperature, and applying various principles of heat transfer[7] (e.g., Fourier's law, Kirchhoff's law), it can be shown that

$$\rho c_p \frac{\partial T}{\partial t} = \frac{1}{r^m}\frac{\partial}{\partial r}\left(r^m k \frac{\partial T}{\partial r}\right) + \pi K(I_T + I_R) - 2\pi n^2 K I_b \tag{11}$$

Notice that the three terms on the right side of Eq. (11) correspond to contributions from conduction along with internal absorption and emission of radiation. Since the energy balance only recognizes gains or losses, scattering doesn't directly appear in the energy expression. Coupled to this expression, however, are the radiation transfer relations. Substituting these relations, Eqs. (6) and (7), into Eq. (11), it is found that

$$\rho c_p \frac{\partial T}{\partial t} = \frac{1}{r^m}\left\{\frac{\partial}{\partial r}\left(r^m k \frac{\partial T}{\partial r}\right) - 2r^m \pi n^2 K I_b + b^m \pi K[2\bar{C}_2 - \bar{C}_1 + 2S\bar{C}_1(y + a)]\right\} \tag{12}$$

As mentioned previously, the incident radiative flux within the material is considered to be much larger than the emitted flux. Thus, it would be expected that

$$(I_T + I_R) >> 2n^2 I_b \tag{13}$$

In other words, the energy loss due to in-depth emission is negligible, and the differential equation becomes

$$\frac{\partial T}{\partial t} = \frac{k}{\rho c_p}\left\{\frac{1}{r^m}\frac{\partial}{\partial r}\left(r^m \frac{\partial T}{\partial r}\right) + \left(\frac{b^m}{r^m}\right)\frac{\pi}{k} K[2\bar{C}_2 - \bar{C}_1 + 2S\bar{C}_1(y + a)]\right\} \tag{14}$$

Boundary Conditions

As previously stated, the exposure surface is subjected to an incident heat flux that is made up of both convective and radiative components. The exact makeup of the incident flux (i.e., spectral characteristics) depends upon many coupled parameters such as, vehicle geometry, entry trajectory, and atmospheric composition. Attaining an accurate assessment of the flowfield conditions for highly energetic, hypervelocity flight, is difficult at best. Suffice it to say, however, that there are methods (i.e., the RASLE[8] code) to do this, and in general, the radiative flux will consist of various spectral bands. For a given material, these bands can be divided into two groups: 1) bands that penetrate the exposed surface and are back-scattered in depth, and perhaps are reflected and/or absorbed by the substrate surface; and 2) bands that do not penetrate the exposed surface and are partially reflected and strongly surface-absorbed. In other words, there are spectral bands to which the surface acts as a window, and others to which it does not. The incident radiative flux can be redefined as

$$q_r = \sum_\nu q_{e_\nu} + \sum_j q_{SNP_j} \tag{15}$$

where the first summation corresponds to the surface-penetrating flux, and the second corresponds to the nonpenetrating flux. Since the nonpenetrating flux never actually enters the material, this flux (actually the absorbed portion of it) only affects the boundary condition. Moreover, at the wavelengths to which the surface is opaque, the surface emits as a black body (with an emittance equal to the absorptance)[9] at the surface temperature. At this point it will be assumed that ablation and phase change do not occur. This is valid as long as the temperature near the exposed surface is not allowed to exceed the melting temperature of the material. At the exposed surface, there is energy (heat) input, as a result of the convective flux plus the surface-absorbed nonpenetrating radiative flux, and energy loss from the surface emission, therefore

$$\frac{\partial T(b, t)}{\partial t} = \frac{1}{k}\left[q_w + \sum_j (q_{SNP_j} - q_{b_j})(1 - R_{e_j})\right] \tag{16}$$

At the rear surface (the substrate/heatshield interface) it is assumed that the temperature remains constant so that

$$T(a, t) = T_0 \tag{17}$$

At zero time, the temperature is presumed to be uniform:

$$T(y, 0) = T_0 \tag{18}$$

Equation (14) can now be further simplified to a tractable partial differential equation by utilizing certain variable transformations. These transformations are geometry dependent, so from here on, the analysis will focus strictly on a spherical configuration. Rewriting Eq. (14) for the spherical case, and generalizing the expression to include spectral detail, yields

$$\frac{\partial T}{\partial t} = \frac{k}{\rho c_p}\left\{\frac{1}{r^2}\frac{\partial}{\partial r}\left(r^2 \frac{\partial T}{\partial r}\right) + \left(\frac{b^2}{r^2}\right)\frac{\pi}{k} \cdot \sum_\nu K_\nu[2\bar{C}_{2_\nu} - \bar{C}_{1_\nu} + 2S_\nu \bar{C}_{1_\nu}(y + a)]\right\} \tag{19}$$

Next let

$$Z \equiv r\sqrt{\frac{\rho c_p}{k}} \tag{20}$$

$$A \equiv a\sqrt{\frac{\rho c_p}{k}} \tag{21}$$

$$B \equiv b\sqrt{\frac{\rho c_p}{k}} \tag{22}$$

$$\Phi \equiv (T - T_0)Z \tag{23}$$

$$\alpha \equiv \left(\frac{2b^2\pi}{\sqrt{k\rho c_p}}\right)\sum_\nu K_\nu S_\nu \bar{C}_{1_\nu} \tag{24}$$

$$\beta \equiv \left(\frac{b^2\pi}{k}\right)\sum_\nu K_\nu(2\bar{C}_{2_\nu} - \bar{C}_{1_\nu}) \tag{25}$$

$$f_b \equiv \left(\frac{1}{\sqrt{k\rho c_p}}\right)\left[q_w + \sum_j (q_{SNP_j} - q_{b_j})(1 - R_{e_j})\right] \tag{26}$$

$$\bar{C}_{1_\nu} = \frac{(q_{e_\nu}/\pi)(1 - R_{e_\nu})(1 - R_{s_\nu})}{\{(1 - R_{i_\nu})[1 + (1 - R_{s_\nu})S_\nu\delta] + R_{i_\nu}(1 - R_{s_\nu})\}} \tag{27}$$

$$\bar{C}_{2_\nu} = \frac{(q_{e_\nu}/\pi)(1 - R_{e_\nu})[1 - (1 - R_{s_\nu})S_\nu a]}{\{(1 - R_{i_\nu})[1 + (1 - R_{s_\nu})S_\nu\delta] + R_{i_\nu}(1 - R_{s_\nu})\}} \tag{28}$$

The differential equation [Eq. (19)], the boundary conditions [Eqs. (16) and (17)], and the initial condition [Eq. (18)] become

$$\Phi_t(z, t) = \Phi_{zz}(z, t) + \alpha + (\beta/Z) \tag{29}$$

$$\Phi_z(B, t) = Bf_b + [\Phi(B, t)/B] \tag{30}$$

$$\Phi(A, t) = 0 \tag{31}$$

$$\Phi(z, 0) = 0 \tag{32}$$

Solution

To solve this set of equations and obtain an expression for the time-dependent temperature distribution, $\Phi(z, t)$ can be divided into "transient" and "steady-state" components:

$$\Phi(z, t) = Y(z, t) + \Psi(z) \tag{33}$$

Taking the various partial derivatives of this expression and substituting into Eqs. (29–32) yields

$$Y_t(z, t) = Y_{zz}(z, t) + \Psi_{zz}(z) + \alpha + (\beta/Z) \tag{34}$$

$$\Psi_z(B) = Bf_b + [\Psi(B)/B] \tag{35}$$

$$Y_z(B, t) = [Y(B, t)/B] \tag{36}$$

$$Y(A, t) = -\Psi(A) \tag{37}$$

$$Y(z, 0) = -\Psi(z) \tag{38}$$

After suitable integration and substitution, the steady-state component is found to be

$$\Psi(z) = \beta Z\left[\ell n\left(\frac{A}{Z}\right)\right] - (Z - A)\frac{\alpha Z}{2} + \left(\frac{Z - A}{A}\right)\left\{B\left[\beta + B\left(f_b + \frac{\alpha}{2}\right)\right]\right\} \quad (39)$$

Next, using the separation-of-variables technique,[10] and utilizing principles of superposition, orthogonality, etc., the transient component is found to be

$$Y(z, t) = \sum_{n=1}^{\infty} C_n \sin[\lambda_n(Z - A)]\exp(-\lambda_n^2 t) \quad (40)$$

Finally, the general solution is

$$T(z, t) = T_0 + \left\{\frac{1}{Z}\sum_{n=1}^{\infty} C_n \sin[\lambda_n(Z - A)]\exp(-\lambda_n^2 t)\right\} + \beta\left[\ell n\left(\frac{A}{Z}\right)\right] - (Z - A)\frac{\alpha}{2} + \left(\frac{Z - A}{ZA}\right)\left\{B\left[\beta + B\left(f_b + \frac{\alpha}{2}\right)\right]\right\} \quad (41)$$

where the series coefficient and eigenvalues are, respectively

$$C_n = \frac{-2\int_A^B \Psi(z)\sin[\lambda_n(Z - A)]\,dz}{\{(B - A) - B\cos^2[\lambda_n(B - A)]\}} \quad (42)$$

$$\lambda_n = \frac{1}{B}\tan[\lambda_n(B - A)] \quad (43)$$

Notice that the general solution, plus the series coefficient and eigenvalue expressions, are in terms of products, summations, and quadratures of known functions. Thus, this solution is exact, and convergence is assured. A computer code has been written for utilizing this solution, and some illustrative cases will now be discussed.

Discussion

Selection of Materials

Using data reported by Dickinson[11] and others,[12] we compared the properties of many potentially useful materials such as KBr, GaAs, CdTe, ZnSe, CaF_2, and KCl. Zinc selenide (ZnSe) was found to have many characteristics that would make it a potentially useful volume-reflecting, thermal protective material. It has a very low-absorption coefficient ($K = 0.005\ \text{cm}^{-1}$) over a broad range of wavelengths. By adjustment of the particle size, in consideration of the anticipated predominant spectral bands (wavelengths), a scattering coefficient as high as $800\ \text{cm}^{-1}$ can reasonably be attained. Furthermore, Fig. 2 (adapted from Magee[13]) shows that ZnSe displays distinctive "window-like" behavior, as discussed in the introduction. The experimental measurements shown in Fig. 3 (adapted from Ref. 8) for two grades of ZnSe, support the notion that material properties can be treated as rather invariant with temperature. In short, ZnSe is a good candidate material in that it displays high-scattering and low-absorbing behavior, and it conforms to the assumptions stipulated in the analytical development.

Before proceeding with the illustrative examples, a couple of comments on selecting the various reflectances are in order. These comments pertain only to surface-penetrating spectral bands. As implied earlier, the heat shield material (in its assembled form) is an open matrix of densely packed scattering particles immersed in a parent medium, presumed to be similar to the atmospheric gases surrounding the heat shield during heating. It would be expected for this case that the reflectance for both the inward- and outward-bound intensities (at the exposed surface) would be effectively zero, that is, $R_e = R_i = 0$, which is both reasonable and conservative. The substrate surface, however, can be chosen to be anything from a nontransmitting black-body absorber ($R_s = 0$) to a perfect mirror ($R_s = 1.0$). In order to gain some insight as to how selection of this parameter affects the results, overall reflectance is defined as the ratio of the net reflected intensity to the incident intensity. Considering surface-penetrating spectral bands only

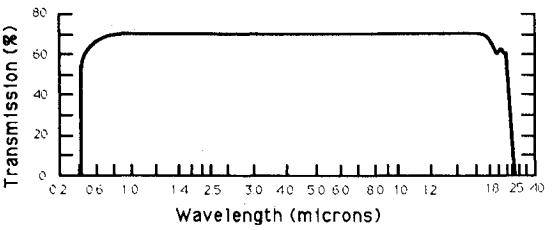

Fig. 2 Transmission characteristics of zinc selenide, 7-mm thick.

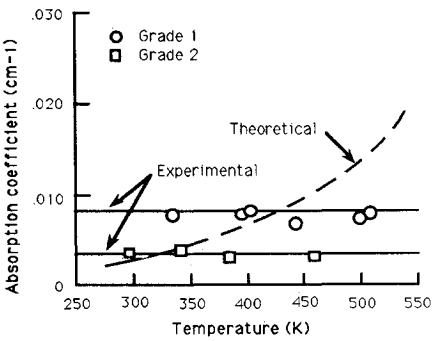

Fig. 3 Variation of absorption with temperature for zinc selenide (at $\lambda = 10.6\ \mu$).

$$R = (I_{Rb}/I_e)$$

which, when combined with previously stated expressions and assumptions, is equivalent to

$$R = 1 - \frac{(1 - R_s)}{1 + (1 - R_s)S\delta}$$

This is the "volume reflectance" of the entire scattering medium for radiation that penetrates the material. Notice that as the substrate surface reflectance R_s approaches unity (i.e., for a perfect mirror) the overall reflectance approaches unity as well. Moreover, as R_s goes to zero (as for a black body) the overall reflectance becomes

$$R = [S\delta/(1 + S\delta)]$$

For this situation it is clear, that the overall reflectance is governed by the magnitude of the scattering coefficient and the material thickness. For the case of ZnSe ($S = 800\ \text{cm}^{-1}$), virtually any coating of reasonable thickness should be an effective "volume reflector" and should be relatively insensitive to the substrate reflectance (i.e., for $\delta \approx O[0.1\ \text{cm}]$, R is near unity).

Illustrative Examples

Consider a ZnSe heat shield that is at a uniform initial temperature of 300 K, is 10-cm thick, and has an inner surface radius of curvature, a, of 100 cm. Suppose that the heat shield is exposed to a constant total heat flux of $400\ \text{W/cm}^2$, that is made up of a convective component, q_w, of $100\ \text{W/cm}^2$, and

a radiative component, q_r, of 300 W/cm^2. For the first case, let us examine the situation where the radiative flux can be lumped into a single spectral band that fully penetrates the exposed surface. In other words, the material and the radiative flux are perfectly matched so that $q_e = q_r = 300$ W/cm^2 and $q_{SNP} = 0$ W/cm^2. The transient material response (temperature distribution at different time intervals) for this situation is shown in Fig. 4.

The exposed surface reaches the melting temperature (≈1400 K) in approximately 40 s. Figure 5 shows the temperature distribution throughout the material at this point in time, along with the relative contributions of the convective and radiative components. Notice that the temperature increase throughout the material, is dominated by the convective heating component, even though the radiative flux is three times larger. This is the primary virtue of the backscattering heat shield concept: when the radiative flux and the heat shield material are properly matched, the effects of the heating caused by the enormous radiative component can be practically eliminated, or at least dramatically reduced. Analogous behavior has been documented experimentally for Teflon®.[14]

Notice also that at 40 s the convective flux only penetrates (by means of conduction) 6 cm into the material. The slight temperature increase beyond this point, is due to the absorbed radiative flux, which travels at the speed of light.

Finally, to verify the assumption that this system is insensitive to the substrate surface reflectance, the case was repeated using $R_s = 1.0$. The only effect was a slight temperature increase (10–15 K) in the last couple of centimeters. Thus the assumption appears to be valid.

The situation remains much the same for the second case. In this case, however, the radiative flux is split into two spectral bands where half of the flux penetrates the exposed surface ($q_e = 150$ W/cm^2) and half does not ($q_{SNP} = 150$ W/cm^2) (wavelengths outside the "window" of Fig. 2). Figure 6 shows how the surface reflectance, R_e (for the nonpenetrating flux), affects the material response. Notice that the absorption of radiation on the exposed surface increases the surface temperature. In fact, for a surface that is fully opaque and nonreflecting ($R_e = 0$) for the nonpenetrating flux, it only takes 7 s for the surface to reach the melting temperature. This situation is effectively the same as having a proportionately larger convective flux (i.e., $q_w = 250$ W/cm^2).

For further comparison (Fig. 7), the temperature distribution at $t = 40$ s for the highly reflective exposed surface situation ($R_e = 0.9$ for $q_{SNP} = 150$ W/cm^2 and $q_e = 150$ W/cm^2) is compared to the initial case ($q_e = 300$ W/cm^2, $q_{SNP} = 0$ W/cm^2).

Notice that the volume reflector (initial case) is slightly better than the partial surface reflector. In order for the radiation heat shield to remain effective, in the event that there is a sizable nonpenetrating flux component, it is important that the surface be highly reflective to this spectral band.

These illustrative examples exercise the analytical formulation, and demonstrate some of the main features of a radiation-backscattering heat shield. It should be recognized that although only two spectral bands are considered, the analytic solution is not limited to this case. Any number of bands, both surface-penetrating and nonpenetrating, each with its own set of reflectances and/or scattering coefficient, absorption coefficient, etc., can be accommodated. The only major limitation is the availability of detailed information on the properties of materials.

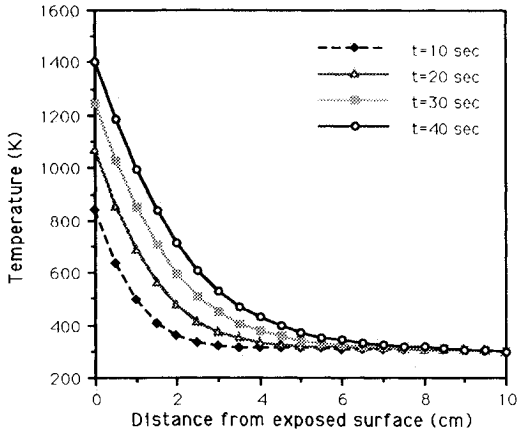

Fig. 4 Transient temperature response, $q_w = 100$ W/cm^2, $q_e = q_r = 300$ W/cm^2, $R_e = R_i = R_s = 0$, $K = 0.005$ cm^{-1}, and $S = 800$ cm^{-1}.

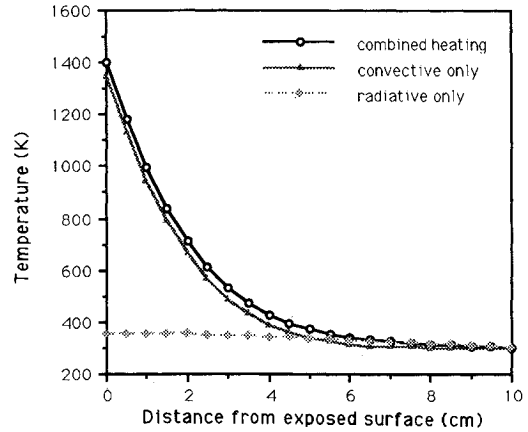

Fig. 5 Temperature distribution at $t = 40$ s, $q_w = 100$ W/cm^2, $q_e = q_r = 300$ W/cm^2, $R_e = R_i = R_s = 0$, $K = 0.005$ cm^{-1}, and $S = 800$ cm^{-1}.

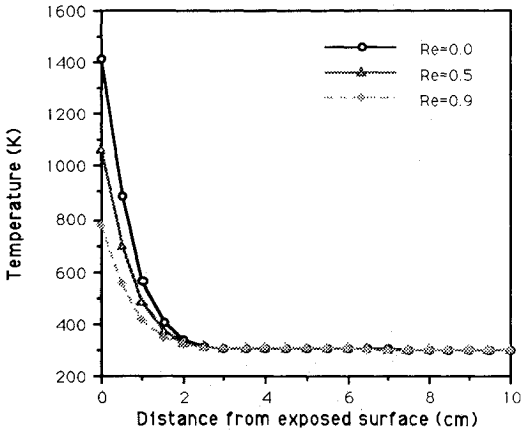

Fig. 6 Effect of surface reflectance on temperature distribution at $t = 7$ s, $q_w = 100$ W/cm^2, $q_e = 150$ W/cm^2, $R_i = R_s = 0$, $q_{SNP} = 150$ W/cm^2, $K = 0.005$ cm^{-1}, and $S = 800$ cm^{-1}.

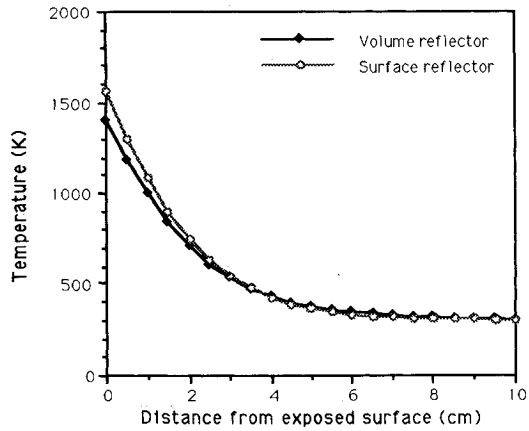

Fig. 7 Temperature distribution at $t = 40$ s for a volume reflector ($q_e = 300$ W/cm^2 and $q_{SNP} = 0$ W/cm^2) and a partial surface reflector ($q_e = 150$ W/cm^2, $q_{SNP} = 150$ W/cm^2, and $R_e = 0.9$).

Conclusions

An analytic solution describing the material response of a radiation-backscattering heat shield exposed to combined convective and radiative heating has been presented. The formulation yields a closed-form, exact solution to the coupled radiative transfer and transient energy equations. The analysis allows for unlimited spectral detail, but assumes that the material properties are essentially invariant with temperature, that the exposed surface doesn't ablate, and that scattering within the material dominates over absorption. The exposed-surface boundary condition allows for convective heating and spectral radiation, some of which penetrates the surface and some of which is absorbed by the surface.

To exercise the analytic development, illustrative examples using a spherical ZnSe heat shield subjected to a radiation-dominated ($q_r = 3q_w$) heating environment were presented. It was shown that if a material is judiciously selected (in consideration of the spectral characteristics of the incident radiative flux) the majority of the flux can be rejected through volume reflection. Furthermore, for cases in which there are significant exposed surface-penetrating and nonpenetrating spectral bands, selecting a good volume-reflecting material that is also highly reflective to the nonpenetrating flux, preserves the effectiveness of the radiation heat shield. Although this formulation is somewhat restrictive in its range of applicability (it does not allow for ablation, and it assumes temperature-invariant material properties), it is an effective tool in providing insight for evaluating the potential effectiveness of a material for radiation-backscattering thermal protective application.

As man continues the ambitious undertaking of exploring the cosmos and utilizing space and its resources, severe radiation-dominated heating environments will almost certainly become more prevalent. Development of radiation-backscattering heat shield technology is therefore a worthwhile pursuit. Acquiring more data on wavelength- and temperature-dependent properties of materials will further this endeavor.

References

[1]Nachtsheim, P. R., Peterson, D. L., and Howe, J. T., "Reflecting and Ablating Heat Shields for Radiative Environments," *The Outer Solar System,* American Astronautical Society, Vol. 29, No. 2, 1971, pp. 253–264.

[2]Brumberger, H., Stein, R. S., and Rowell, R., "Light Scattering," *Science and Technology,* Vol. 1, Nov. 1968, pp. 34–42.

[3]Kubelka, P., and Munk, R., "Ein Beitrag zur Optik der Farhenstriche," *Zeitschrift Für Technische Physik,* Vol. 12, 1931, p. 593.

[4]Howe, J. T., and Yang, L., "Thermal Protection for Hypervelocity Flight in Earth's Atmosphere by Use of Radiation Backscattering Ablating Materials," AIAA Paper 91-1321, June 1991.

[5]Schuster, A., "Radiation Through a Foggy Atmosphere," *Astrophysical Journal,* Vol. 21, No. 1, 1905, pp. 1–22.

[6]Reynolds, W. C., and Perkins, H. C., *Engineering Thermodynamics,* 2nd ed., McGraw-Hill, New York, 1977, Chap. 5, pp. 105–143.

[7]Kreith, F., and Black, W. Z., *Basic Heat Transfer,* 1st ed., Harper & Row, New York, 1980.

[8]Nicolet, W. E., and Balakrishnan, A., "Radiating Shock Layer Environment, RASLE, (User's Manual)," Acurex Rept. UM-79-10/AS, Mountain View, CA, July 1979.

[9]Viskanta, R., "Radiation Transfer and Interaction of Convection with Radiation Heat Transfer," *Advances in Heat Transfer,* 1st ed., Vol. III, Academic Press, New York, 1966, pp. 176–251.

[10]Churchhill, R. V., and Brown, J. W., *Fourier Series and Boundary Value Problems,* 4th ed., McGraw-Hill, New York, 1987, Chap. 2, pp. 36–49.

[11]Dickinson, S. K., "Infrafed Laser Window Materials Property Data for ZnSe, KCl, NaCl, CaF2, SrF2, BaF2," AF Cambridge Research Lab. Rept. AFCRL-TR-75-0318, Cambridge, MA, June 1975.

[12]"Zinc Selenide Optics," *Coherent Radiation Catalog,* Coherent Co., Palo Alto, CA, 1973, pp. VI–VII.

[13]Magee, T. J., et al., "Compact Calorimeter for Measuring Laser Absorption Coefficients of Small Samples," *Review of Scientific Instruments,* Vol. 47, No. 3, 1976, p. 301.

[14]Howe, J. T., Green, M. J., and Weston, K. C., "Thermal Shielding by Subliming Volume Reflectors in Convective and Intense Radiative Environments," *AIAA Journal,* Vol. II, No. 7, 1973, pp. 944–989.